10.1109/ISNE.2019.8896544

The 8th IEEE International Symposium on Next-Generation Electronics (ISNE 2019)

Equivalent Circuit Models for Next Generation Photovoltaic Devices with S-shaped I-V Curves

Francisco J. García-Sánchez *
Superior School of Experimental Sciences and Technology
Universidad Rey Juan Carlos
Madrid, Spain,
franciscojavier.garcia.sanchez@urjc.es

Beatriz Romero
Superior School of Experimental Sciences and Technology
Universidad Rey Juan Carlos
Madrid, Spain.
beatriz.romero@urjc.es

***Abstract*— Certain still un-optimized emergent photovoltaic devices that are being developed for next generation solar cell applications exhibit under illumination an unwanted *S*-shaped concave kink in their current-voltage characteristics that substantially hinders the photovoltaic device's energy conversion efficiency. This anomalous behavior shows up in the *I-V* curves of several kinds of solar cells, such as some organic cells and various other types of still evolving devices, which are promising potential candidates for future photovoltaic applications. The underlying physical phenomena responsible for the detrimental *S*-shaped kink can be conveniently modeled using lumped-parameter equivalent circuits that adequately replicate the illuminated *S*-shaped *I-V* characteristics. We review and discuss here the most prominent types of those equivalent circuit model configurations.**

Keywords*— solar cells, next-generation photovoltaic devices, equivalent circuit model, S-shaped kink, organic solar cells.

I. INTRODUCTION

Solar cells (SCs) traditionally have been represented under dark and illumination conditions by equivalent circuit models whose defining equations mathematically describe their current-voltage (*I-V*) characteristics. Such circuits consist of combinations of interconnected discrete active and passive lumped elements, whose parameter values attempt to compactly represent the most significant physical phenomena of the solar cell. They are convenient tools to optimize the design of SCs and SC arrays. A full overview of conventional SCs' equivalent circuit models is presented in [1].

Practical adoption of emergent photovoltaic devices as potentially viable candidates for next-generation SCs sometimes is obstructed by the presence of undesirable features that hamper the energy conversion process. A most troubling occurrence is the presence of an illumination intensity-dependent *S*-shaped kink in the power-producing fourth (also the first) quadrant of the *I-V* characteristics of some developmental solar cells while they are still un-optimized, or when they have deteriorated [2]. Such *S*-shaped kinks are typically observed in the *I-V* curves of certain classes of emergent photovoltaic devices, such as small molecule and polymeric bulk heterojunction in normal and inverted organic solar cells (OSCs) [2]-[7]. They also show up in some other types of unconventional amorphous, inorganic and hybrid solar cells [8]-[13] that are potential candidates for next-generation photovoltaics. An illustrative example of what an *S*-shaped kink looks like is shown in Fig. 1, for an experimental OSC [14]. The presence of the *S*-shaped kink

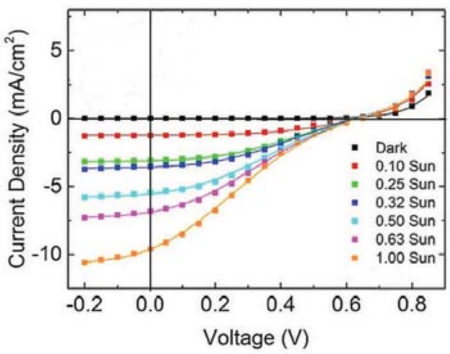

Fig. 1. Illumination intensity-dependent S-shaped *I-V* characteristics, measured (symbols) and modeled (lines) from an experimental PBDTTT-CF:$PC_{71}BM$-based OSC (described in [14]).

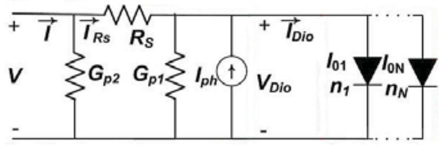

Fig. 2. A generic lumped-parameter (condensed element) equivalent circuit to model conventional solar cells. Elements include: an illumination dependent photo-current source, multiple parallel diodes to represent more than one significant junction conduction mechanism, at least one series resistor to account for the carrier collection electrodes parasitic resistance, and two parallel conductors to account for the possibile presence of both peripheral and bulk parasitic resistive shunt losses, as described in [1].

may be attributed to several causes [15], [16]; among them, thickness, interlayer resistance [17], a strong imbalance of charge carrier mobilities [18], surface recombination, voltage dependent dipoles and traps that create energy barriers for carrier injection and extraction at the contacts [3]-[5], [19]-[22], etc. This type of kink must be avoided at all costs, because its presence severely limits the *I-V* curve's fill factor (*FF*) [23], even down to values below 50%, which in turn drastically reduces the cell's energy conversion efficiency capability. Thus, whenever *S*-shaped kinks are observed under illumination in the *I-V* curves of potentially useful emergent photovoltaic devices, design optimization actions must be undertaken to prevent or suppress the presence of such kinks.

II. DESIGN OPTIMIZATION

Optimization involves effectively removing or modifying the *material, structural* or *processing* aspects of a prototype device that might cause the *S*-shaped kink, either initially or as a consequence of ageing deterioration. Hence, to begin with, the specific culprit phenomena or feature must be effectively identified through proper follow up and analysis.

Work partly supported by Spain's Ministry of Science, Innovation and Universities Project No. TEC2016-77242-C3-3-R.

Lumped-parameter equivalent circuit SC models are perfectly suited analytical tools for that purpose. However, the occurrence of *S*-shaped kinks in *I-V* curves demands the use of more elaborated circuit model configurations than those available for conventional SCs, whose generic structure is pictured in Fig. 2 [1]. SCs with *S*-shaped *I-V* curves require equivalent circuit models with specialized lumped elements to purposely describe each significant physical phenomenon believed to cause the abnormal *S*-shaped kink behavior in the *I-V* curves [23].

III. Equivalent Circuit Model Configurations

There are various lumped-parameter circuit configurations that can be used to model the *I-V* curves of SCs with *S*-shaped kinks. They all consist of inserting additional lumped-parameter circuit elements into a conventional SC equivalent circuit model configuration, generally a single diode version of that shown in Fig. 2. The most commonly used types may be classified essentially into two broad categories.

A. Modifications of the conventional SC model

The earliest lumped-parameter circuit model specifically intended to account for the *S*-shaped kink most likely was that originally proposed by Mazhari in 2006 [24], shown in Fig. 3. It is made up of the simplest conventional SC equivalent circuit model comprised of one diode in parallel with the photocurrent source, modified by the addition of two other diodes. One of them, D_{ext}, is connected in series back-to-back with diode D_{rec}, which is in parallel with the photocurrent source. The second diode D_{dark}, is placed in parallel with the terminals, as shown in Fig. 3.

A related form of modification of the conventional SC circuit model is represented by the so-called back-to-back diode model (B2BDM), proposed in 2018 by Sensa et al [25], shown in Fig. 4. In this equivalent circuit the complete series combination of the two back-to-back diodes, D_1 and D_2, is placed in parallel with the photocurrent source I_L and a shunt resistor R_{P1}. The outstanding feature of this model is that it

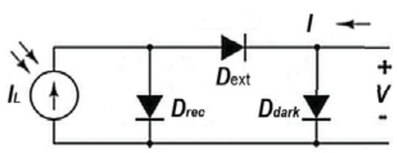

Fig. 3. Original equivalent circuit model suggested in 2006 by Mazhari [24] to represent the detrimental *S*-shaped kink in the *I-V* characteristics under illumination.

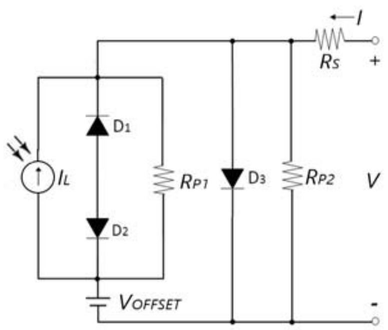

Fig. 4. Back-to-back diodes in parallel with a shunt resistor and the photo-current source, all in series with an offset voltage source, and then connected in parallel to another diode and shunt resistor, again in series with a resistor, as proposed in 2018 by Sensa et al [25], [26].

includes a displacement along the voltage axis, achieved by inserting a series offset voltage source V_{OFFSET}. The complete assembly is then connected in parallel to a third diode D_3 and a shunt resistor R_{P2}, completed by a resistor R_S placed in series with the terminals, as shown in Fig. 4. [25], [26].

It is convenient for practical purposes being able to find closed-form explicit solutions of the mathematical equation set that describes the circuit model. Not only do they facilitate simulation, but also simplify fitting the cell's measured *I–V* data to extract the model's elements' parameter values. Closed-form solutions of Mazhari's equivalent circuit model equations have been obtained [14], [27]. Some further refinements that increase the descriptive ability of Mazhari's original model, include inserting resistors in parallel with either diode D_{rec} [28], or diode D_{dark} [29], or with both [30], and even with diode D_{ext} [31].

B. Additions in series with conventional SC models

Another category of equivalent circuit configuration consists of connecting additional sub-circuits containing voltage dependent elements in series with a conventional SC equivalent circuit model to produce the expected *S*-shaped kink in the *I-V* curve. The simplest solution, shown in Fig. 5.a, would be to insert an undetermined generic voltage-dependent series resistor, as suggested in [32]. Although simple, this model might not be the most convenient in practice, because of the presence of the undetermined circuit element.

Alternatively, a voltage dependent behavior may be included using some appropriate combinations of diodes and constant resistors. Such is the configuration originally proposed by De Castro et al in 2010 [15] for an additional sub-circuit 2: a parallel combination of one diode and a resistor, as shown in Fig. 5.b. A closed-form explicit solution of this circuit's implicit equations based on the Lambert W-function was proposed in 2012 [33] and used for direct extraction of the model elements' parameter values [34], [35]. Another solution was proposed in 2013 using Special Trans Functions Theory (STFT) [36]. The analytical solution was again later improved in 2016 by De Castro et al [37].

The circuit model proposed by De Castro et al [15], shown in Fig. 5.b, represents an outstanding step, because it satisfactorily reproduces the *S*-shaped kink within the power-producing fourth quadrant of the illuminated *I-V* characteristics. Unfortunately, however, it cannot adequately describe the *I-V* curve beyond the open-circuit point in the first quadrant, where the current of many practical devices often keep on growing, describing an exponential-like upward turn.

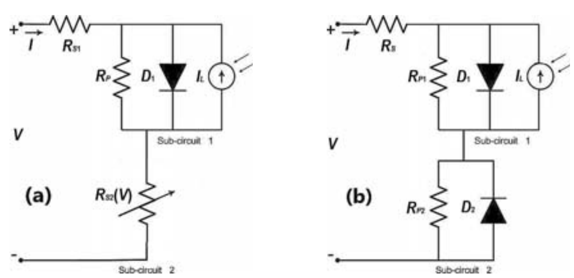

Fig. 5. A conventional solar cell one-diode (upper sub-circuit 1) model with photocurrent source and parallel and series resistors is connected in series to a (lower) sub-circuit 2 consisting of: (a) a generic voltage controlled resistor, as suggesteded in [32], and (b) a single diode in parallel with a resistor, as originally proposed in 2010 by De Castro et al [15].

Although the first quadrant would seem at first to lack modeling interest because it is not a power-producing region, it is advantageous to be able to model all significant physical phenomena in all the three regions where they are manifested, including the first quadrant of the illuminated *I-V* characteristics.

To account for the observed behavior in the first quadrant, García-Sánchez et al proposed in 2013 [38] an enhancement of the original De Castro et al circuit model [15]. The R_{P2} resistor present in the lower sub-circuit 2 of that original model is replaced by another diode D_3 placed in the forward direction, so that an anti-parallel diode pair D_2-D_3 results, as shown in Fig. 6.a. The effect of the D_2-D_3 pair on the *I-V* curve is very conspicuous, as can be seen from the graphical comparison, shown in Fig. 7, of the De Castro et al original circuit (Fig. 5.b) and the García-Sánchez et al circuit (Fig. 6.a), both fitted to the same set of *I-V* data, from an illuminated OSC that exhibits exponential-like rise of its *I-V* curve in the first quadrant beyond the open-circuit voltage point. That upward turn is reproduced well in the fourth quadrant by both models, but only so in the first quadrant by the García-Sánchez et al model. Zuo et al proposed in 2014, through comparable reasoning, the use of an extra rectifying junction in the sub-circuit of this model [19]. Further enhancements of this circuit model were proposed in 2016 by De Castro et al [37] and by Ronald et al [39]. The parallel resistor R_{P2} of the lower sub-

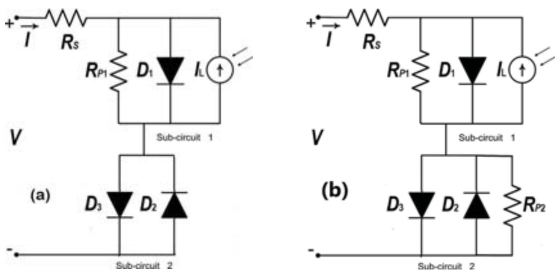

Fig. 6. Improvements to the original De Castro et al [15] circuit: (a) the model proposed in 2013 by García-Sánchez et al [38], where the resistor in the lower sub-circuit of the De Castro et al circuit is replaced by a diode, resulting in an anti-parallel diode pair, and (b) a further refinement proposed in 2016 [37], [39], where the shunting resistor is again included in parallel with the anti-parallel diode pair in the lower sub-circuit of the García-Sánchez et al model.

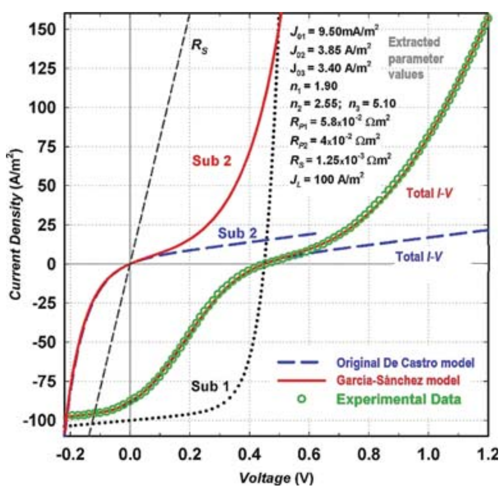

Fig. 7. A comparison of the De Castro et al [15] circuit model (blue), shown in Fig. 5.b, and the García-Sánchez et al [38] circuit model (red), shown in Fig. 6.a, both fitted to actual experimental data (green symbols) measured under illumination, with a distinct exponential-like upward turn in the first quadrant of the *I-V* curve.

circuit 2 (Fig. 5.b), which was replaced by the forward conducting diode D_3 (Fig. 6.a) by García-Sánchez et al [38], was brought back to be connected in parallel with the anti-parallel diode pair D_2-D_3 (Fig. 6.b). This addition restores the account of the shunt loss path across the bulk of the cell, thus providing increased descriptive flexibility, including a better account of the *I-V* curve slope around the open-circuit voltage point. Laudani et al [40] studied the illumination intensity dependence of this model's lumped parameters in OSCs. Yu et al [41] recently derived analytical solutions for the set of equations of these circuit models which facilitate fast and accurate simulation and parameter extraction.

IV. Conclusion

S-shaped kinks present in the *I-V* characteristics of some types of emergent photovoltaic devices, with good potential as candidates for next-generation SC applications, seriously reduce their power conversion efficiency. We have reviewed the lumped-parameter (condensed elements) equivalent circuit models that can be used to portray the underlying physical phenomena that cause *S*-shaped kinks [23]. They are effective analytical tools to probe structural, material, and phenomenological aspects of emergent devices. Observation and follow up of the circuit model elements' parameter values provide insight for identifying the causes of such *S*-shaped behavior. That knowledge allows establishing guidelines for overcoming or minimizing the *S*-shaped kinks during design optimization of emerging solar cell technologies [42].

Acknowledgment

We appreciate the contributions and support of B. Arredondo, G. del Pozo, J.J. Liou, J. Muci, D. Lugo-Muñoz, A. Ortiz-Conde, and A. Sucre-González.

References

[1] A. Ortiz-Conde, F. J. García-Sánchez, J. Muci, A. Sucre-González, "A review of diode and solar cell equivalent circuit model lumped parameter extraction procedures," *Facta Univer: Electron & Energ*, vol. 27, no. 1, pp. 57–102, Mar 2014. doi: 10.2298/FUEE1401057O

[2] A. Wagenpfahl, D. Rauh, M. Binder, C. Deibel, V. Dyakonov. "S-shaped current-voltage characteristics of organic solar devices," *Phys Rev B*, vol. 82, no. 11, art. 115306, Sep 2010. doi: 10.1103/PhysRevB.82.115306

[3] A. Kumar, S. Sista, Y. Yang, "Dipole induced anomalous S-shape I-V curves in polymer solar cells," *J App Phys*, vol. 105, art. 094512, May 2009. doi: 10.1063/1.3117513

[4] B. Y. Finck, B. J. Schwartz, B. J. "Understanding the origin of the S-curve in conjugated polymer/fullerene photovoltaics from drift-diffusion simulations," *Appl Phys Lett*, vol. 103, no. 5, art. 053306, p. 143_1, Jul 2013 doi: 10.1063/1.4817396

[5] A. Gusain, R. M. Faria, P. B. Miranda. "Polymer Solar Cells—Interfacial Processes Related to Performance Issues." *Frontiers in chemistry*, vol. 7, art. 61, Feb 2019. doi:10.3389/fchem.2019.00061

[6] G. Lastra, V. S. Balderrama, L. Reséndiz, J. Pallarés, L. F. Marsal, V. Cabrera, M. Estrada, "Air Environment Degradation of a High-Performance Inverted PTB7-Th:PC$_{70}$BM Solar Cell," *IEEE J of Photov*, vol. 9, no. 2, pp. 464–468, Mar 2019. doi: 10.1109/JPHOTOV.2019.2892108

[7] G. del Pozo, B. Romero, B. Arredondo. "Evolution with annealing of solar cell parameters modeling the S-shape of the current–voltage characteristic," *Solar Ener Mat Solar Cells*, vol. 104, pp. 81–86, Sep 2012. doi: 10.1016/j.solmat.2012.04.048

[8] J. Zhao, Y. Xu, F. Ma, A. Ho-Baillie, H. Zhang, S. Bremner. "Simulation of Solar Cells Employing 2 Dimensional Transition Metal Dichalcogenide–Silicon Front Surfaces." In *2018 IEEE 7th World Conf on Photovolt Ener Conver (WCPEC)*, pp. 2092–2096, 10-15 Jun 2018. doi: 10.1109/PVSC.2018.8547793

[9] S. Mudgal, S. Singh, V. K. Komarala, "Investigation of Electrical Parameters of Amorphous–Crystalline Silicon Heterojunction Solar Cells: Correlations Between Carrier Dynamics and S-Shape of Current Density–Voltage Curve," *IEEE J of Photov*, vol. 8, no. 4, pp. 909–915, Jul 2018. doi: 10.1109/JPHOTOV.2018.2821839

[10] M. Ramírez-Como, V. S. Balderrama, A. Sacramento, L. F. Marsal, G. Lastra, and M. Estrada. "Fabrication and characterization of inverted organic PTB7: PC$_{70}$BM solar cells using Hf-In-ZnO as electron transport layer." *Solar Energy*, vol. 181, pp. 386–395, Mar 2019. doi: 10.1016/j.solener.2019.02.015

[11] A. Khatibi, F. Razi Astaraei, M. H. Ahmadi, "Generation and combination of the solar cells: A current model review," *Energy Sci & Eng*, vol. 7, no. 2, pp. 305-322, Apr 2019. doi: 10.1002/ese3.292

[12] T. Ablekim, C. Perkins, X. Zheng, et al, "Tailoring MgZnO/CdSeTe Interfaces for Photovoltaics," *IEEE J of Photov*, vol. 9, no. 3, pp. 888–892, May 2019. doi: 10.1109/JPHOTOV.2018.2877982

[13] M. F. Abdullah, A. M. Hashim, "Review and assessment of photovoltaic performance of graphene/Si heterojunction solar cells," *J Mater Sci*, vol. 54, no. 2, pp. 911–948, Jan 2019. doi: 10.1007/s10853-018-2947-3

[14] B. Romero, G. del Pozo, B. Arredondo, D. Martín-Martín, M. P. Ruiz Gordoa, A. Pickering, A. Pérez-Rodríguez, E. Barrena, F. J. García-Sánchez, "S-Shaped *I–V* Characteristics of Organic Solar Cells: Solving Mazhari's Lumped-Parameter Equivalent Circuit Model," *IEEE Trans Electron Dev*, vol. 64, no. 11, pp. 4622–4627, Nov 2017. doi: 10.1109/TED.2017.2749411

[15] F.A. De Castro, J. Heier, F. Nuesch, R. Hany, 2010. "Origin of the kink in current density versus voltage curves and efficiency enhancement of polymer-C$_{60}$ heterojunction solar cells," *IEEE J Select Topics Quant Electron*, vol. 16, no. 6, pp. 1690–1699, Nov-Dec 2010. doi: 10.1109/JSTQE.2010.2040807

[16] J. Wagner, M. Gruber, A. Wilke, et al, "Identification of different origins for S-shaped current voltage characteristics in planar heterojunction organic solar cells." *J App Phys*, vol. 111, no. 5 art. 054509, Mar 2012. doi: 10.1063/1.3692050

[17] B. Ecker, H.-J. Egelhaaf, R. Steim, J. Parisi, E. von Hauff, "Understanding S-Shaped Current–Voltage Characteristics in Organic Solar Cells Containing a TiOx Interlayer with Impedance Spectroscopy and Equivalent Circuit Analysis," *J of Phys Chem C*, vol. 116, no. 31, pp. 16333–16337, Jul 2012. doi: 10.1021/jp305206d

[18] W. Tress, A. Petrich, M. Hummert, M. Hein, K. Leo, M. Riede. "Imbalanced mobilities causing S-shaped IV curves in planar heterojunction organic solar cells." *App Phys Lett*, vol. 98, no. 6, art. 063301, Feb 2011. doi: 10.1063/1.3553764

[19] L. Zuo, J. Yao, H. Li, H. Chen, "Assessing the origin of the S-shaped *I–V* curve in organic solar cells: An improved equivalent circuit model," *Solar Energy Mater. Solar Cells*, vol. 122, pp. 88–93, Mar 2014. doi: 10.1016/j.solmat.2013.11.018

[20] Tress, W., "Interplay Between Electrodes and Active Materials: The Open-Circuit Voltage and S-shaped J-V Curves," Chaper 6 in *Organic Solar Cells*. Springer Series in Materials Science, vol 208, pp. 315–357, Nov 2014. doi: 10.1007/978-3-319-10097-5_6

[21] Tress, W., "Further Origins of S-shaped J-V Curves," Chaper 7 in *Organic Solar Cells*. Springer Series in Materials Science, vol 208, 359–376, Nov 2014. doi: 10.1007/978-3-319-10097-5_7

[22] B. Romero, G. Del Pozo, E. Destouesse, S. Chambon, B. Arredondo, "Circuital modelling of S-shape removal in the current–voltage characteristic of TiOx inverted organic solar cells through white-light soaking," *Organic Electron*, vol. 15, no. 12, pp. 3546–3551, Dec 2014. doi: 10.1016/j.orgel.2014.09.033

[23] F. J. García-Sánchez, B. Romero, D. C. Lugo-Muñoz, G. del Pozo, B. Arredondo, J. J. Liou, A. Ortiz-Conde, "Modeling solar cell S-shaped *I-V* characteristics with DC lumped-parameter equivalent circuits: A review," *Facta Univers: Electron & Energ*, vol. 30, no. 3, pp. 327–350, Sep 2017. doi: 10.2298/FUEE1703327G

[24] B. Mazhari, "An improved solar cell circuit model for organic solar cells," *Solar Energy Mater. Solar Cells*, vol. 90, no. 7, pp. 1021–1033, 2006, doi: 10.1016/j.solmat.2005.05.017

[25] E. Sesa, B. Vaughan, K. Feron, C. Bilen, X. Zhou, W. Belcher, P. Dastoor, "A building-block approach to the development of an equivalent circuit model for organic photovoltaic cells," *Org Electr*, vol. 58, pp. 207–215, Jul 2018. doi: 10.1016/j.orgel.2018.04.019

[26] E. Sesa, D. Darwis, X. Zhou, W. J. Belcher, P. C. Dastoor, "Experimental determination of the relationship between the elements of a back-to-back diode model for organic photovoltaic cells' S-shaped I-V characteristics and cell structure," *AIP Advances,* vol. 9, art. 025014, Feb 2019. doi: 10.1063/1.5063467

[27] G. Huang, F. Yu, C. Xu, "An analytical solution to lumped parameter equivalent circuit model of organic solar cells," *Crystals*, vol. 8, no. 5, art. 224, May 2018. doi: 10.3390/cryst8050224

[28] C. Xu, F. Yu, W. Lin, G. Huang. "An Improved Organic Solar Cell Lumped-Parameter Equivalent Circuit Model." *Crystals*, vol. 8, no. 7, art. 277, Jul 2018. doi: 10.3390/cryst8070277

[29] F. Yu, G. Huang, W. Lin, C. Xu. "Lumped-Parameter Equivalent Circuit Model for S-Shaped Current–Voltage Characteristics of Organic Solar Cells." *IEEE Trans Electron Dev*, vol. 66, no. 1, pp. 670–677, Jan 2019. doi: 10.1109/TED.2018.2878465

[30] F. Yu, G. Huang, W. Lin, C. Xu, "An analysis for S-shaped *I-V* characteristics of organic solar cells using lumped-parameter equivalent circuit model," *Solar Energy*, vol. 177, pp. 229–240, Jan 2019. doi: 10.1016/j.solener.2018.11.011

[31] T. Wei, C. Xu, W. Lin, G. Huang, F. Yu. "A Lumped-Parameter Equivalent Circuit Modeling for S-Shaped *I–V* Kinks of Organic Solar Cells." *Crystals*, vol. 9, no. 2, art 80, Feb 2019. doi: 10.3390/cryst9020080

[32] A Khorami, M. Joodaki, "Extracting voltage□dependent series resistance of single diode model for organic solar cells," *SN Appl Sci*, vol. 1, art 619, Jun 2019. doi: 10.1007/s42452-019-0613-2

[33] B. Romero, G. del Pozo, B. Arredondo, "Exact analytical solution of a two diode circuit model for organic solar cells showing S-shape using Lambert W-functions," *Solar Energy*, vol. 86, no. 10, pp. 3026–3029, Oct 2012. doi: 10.1016/j.solener.2012.07.010

[34] K. Tada, "Parameter extraction from S-shaped current-voltage characteristics in organic photocell with opposed two-diode model: Effects of ideality factors and series resistance," *Phys Status Solidi (a)*, vol. 212, no. 8, pp. 1731–1734, Aug 2015. doi: 10.1002/pssa.201431877

[35] K. Tada, "Validation of opposed two-diode equivalent-circuit model for S-shaped characteristic in polymer photocell by low-light characterization," *Organic Electron*, vol. 40, pp. 8-12, Jan 2017. doi: 10.1016/j.orgel.2016.10.031

[36] N.S. Singh, A. Jain, A. Kapoor. "Exact analytical solution for organic solar cells showing S-shaped JV characteristics using Special Trans Function Theory (STFT)." *Int. J. Renew Energy Res (IJRER)*, vol. 3, no. 2, pp. 453–457, Jun 2013.

[37] F. De Castro, A. Laudani, F. R. Fulginei, A. Salvini, "An in-depth analysis of the modelling of organic solar cells using multiple-diode circuits," *Solar Energy*, vol. 135, pp. 590–597, Oct 2016. doi: 10.1016/j.solener.2016.06.033

[38] F. J. García-Sánchez, D. Lugo-Munoz, J. Muci, A. Ortiz-Conde. "Lumped parameter modeling of organic solar cells' S-shaped I–V characteristics." *IEEE J. of Photov*, vol. 3, no. 1, pp. 330–335, Jan 2013. doi: 10.1109/JPHOTOV.2012.2219503

[39] P. J. Roland, K. P. Bhandari, R. J. Ellingson, "Electronic Circuit Model for Evaluating S-Kink Distorted Current-Voltage Curves," *Proc. IEEE 43rd Photov Specialists Conf. (PVSC)*, pp. 3091–3094, Nov 2016, doi: 10.1109/PVSC.2016.7750234

[40] A. Laudani, F. R. Fulginei, F. De Castro, A. Salvini, "Irradiance intensity dependence of the lumped parameters of the three-diodes model for organic solar cells," *Solar Energy*, vol. 163, pp. 526–536, Mar 2018. doi: 10.1016/j.solener.2018.02.032

[41] F. Yu, G. Huang, W. Lin, C. Xu, W. Deng, X. Ma, J. Huang, "Lumped-Parameter Equivalent Circuit Modeling of Solar Cells with S-Shaped *I-V* Characteristics," *Solid-State Electron,* vol. 156, pp. 79–86, Jun 2019. doi: 10.1016/j.sse.2019.03.029

[42] R. Saive, "S-Shaped Current–Voltage Characteristics in Solar Cells: A Review," *IEEE Journal of Photovoltaics*, Early Access, Aug 2019. doi: 10.1109/JPHOTOV.2019.2930409